Catalyst Design Hot Paper

DOI: 10.1002/anie.201408222

Molybdenum Phosphosulfide: An Active, Acid-Stable, Earth-Abundant Catalyst for the Hydrogen Evolution Reaction**

*Jakob Kibsgaard and Thomas F. Jaramillo**

Abstract: *Introducing sulfur into the surface of molybdenum phosphide (MoP) produces a molybdenum phosphosulfide (MoP|S) catalyst with superb activity and stability for the hydrogen evolution reaction (HER) in acidic environments. The MoP|S catalyst reported herein exhibits one of the highest HER activities of any non-noble-metal electrocatalyst investigated in strong acid, while remaining perfectly stable in accelerated durability testing. Whereas mixed-metal alloy catalysts are well-known, MoP|S represents a more uncommon mixed-anion catalyst where synergistic effects between sulfur and phosphorus produce a high-surface-area electrode that is more active than those based on either the pure sulfide or the pure phosphide. The extraordinarily high activity and stability of this catalyst open up avenues to replace platinum in technologies relevant to renewable energies, such as proton exchange membrane (PEM) electrolyzers and solar photoelectrochemical (PEC) water-splitting cells.*

Molecular hydrogen (H_2) is one of the world's most important chemicals with a global production rate of approximately 50 billion kg per year and mainly used for petroleum refining and for synthesizing ammonia (NH_3)-based fertilizers.[1] The demand for H_2 may likely increase to feed a growing global population and to process heavier petroleum feedstocks. As hydrogen is mainly produced from fossil fuels, developing an alternative, renewable pathway to produce H_2 in a cost-competitive manner would have a significant impact in reducing fossil-fuel usage and CO_2 emissions. One attractive pathway for clean hydrogen production is through electrochemical processes, such as solar photoelectrochemical (PEC) water splitting or electrolysis, coupled to renewable energy sources, such as wind or solar energy.[2–4]

The hydrogen evolution reaction (HER, $2H^+ + 2e^- \rightarrow H_2$) constitutes half of the water-splitting reaction. To increase process efficiency, active catalysts for the HER are needed. Currently, platinum is the best known HER catalyst as only small overpotentials are required for high reaction rates, but the scarcity and high cost of Pt may limit its widespread technological use. Non-noble-metal alternatives include nickel and nickel alloy catalysts but they are typically not stable in acidic solutions, preventing their use in proton exchange membrane (PEM)-based electrolyzers, which have significant advantages over more conventional alkaline electrolyzers.[5,6]

Very few earth-abundant catalysts have shown efficacy for the HER in strong acids. Nanostructured nickel phosphide,[7] cobalt phosphide,[8] and molybdenum sulfides[9–14] are among the best reported systems, demonstrating high activity for the HER and, for some of these catalysts, excellent stability under these conditions as well. Nickel and cobalt phosphides and molybdenum sulfides further share their efficacy for hydrodesulfurization (HDS) catalysis. The commonalities among catalysts for HDS and HER are not surprising as both reactions rely on the ability of a catalyst to bind an important reactive intermediate, namely hydrogen, in a close to thermoneutral manner. In a HDS reaction, H_2 dissociates on the catalyst surface to react with sulfur to produce H_2S, thereby creating a reactive sulfur vacancy site; in the HER, protons bind to the catalyst to form adsorbed H and ultimately, H_2.[15–18]

Molybdenum phosphide (MoP) is another known HDS catalyst that has recently been shown to be an active HER catalyst;[19–21] herein, we describe that engineering the MoP surface to more closely resemble its state during HDS operating conditions leads to significant enhancements in both catalytic activity and stability for the HER. A number of reports on the HDS reaction indicate that sulfur plays an important role in HDS over transition-metal phosphides.[22–24] For both Ni_2P and MoP, the most active sites are thought to originate from a surface phosphosulfide generated during HDS reactions. To explore if a surface phosphosulfide is also beneficial for the HER, we introduced sulfur in the surface region of the synthesized MoP, which led to remarkable improvements in catalyst performance. MoP with a phosphosulfide surface (MoP|S) exhibits one of the highest HER activities of any non-noble-metal electrocatalyst, while remaining almost perfectly stable in acid.

MoP catalysts supported on titanium foil (geometric area: 0.25 cm^2) were prepared by a wet chemical route as described in the Supporting Information. The surface phosphosulfides were created by a post-sulfidation treatment of MoP in an H_2S atmosphere.

Figure 1A shows the powder X-ray diffraction (XRD) patterns of the as-synthesized molybdenum phosphide with and without the sulfidation treatment. Both diffractograms reveal crystalline MoP (hexagonal, space group $P\bar{6}m2$);[25] the corresponding crystal structure is shown in Figure 1B. The strong similarity between the diffractograms of MoP and MoP|S indicates that the short sulfidation treatment did not significantly alter the bulk crystal structure of MoP.

[*] Dr. J. Kibsgaard, Prof. T. F. Jaramillo
Department of Chemical Engineering, Stanford University
Stanford, CA 94305 (USA)
E-mail: jaramillo@stanford.edu

[**] J.K. and T.F.J. acknowledge support from the US Department of Energy, Office of Science, Office of Basic Energy Sciences (DE-SC0008685).

Supporting information for this article is available on the WWW under http://dx.doi.org/10.1002/anie.201408222.

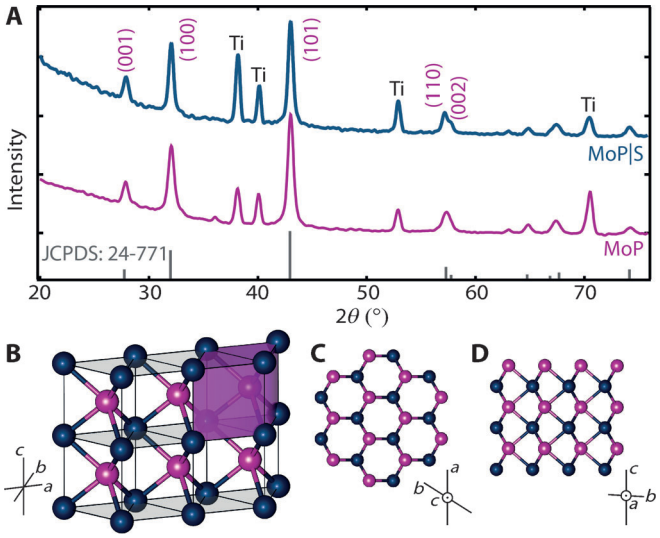

Figure 1. MoP crystal structure. A) XRD patterns of MoP and MoP | S supported on Ti foil with a reference diffractogram of the MoP crystal (JCPDS 24-0771). B–D) Corresponding MoP crystal structure. The purple rhombic prism displays the unit cell. Molybdenum blue, phosphorus magenta.

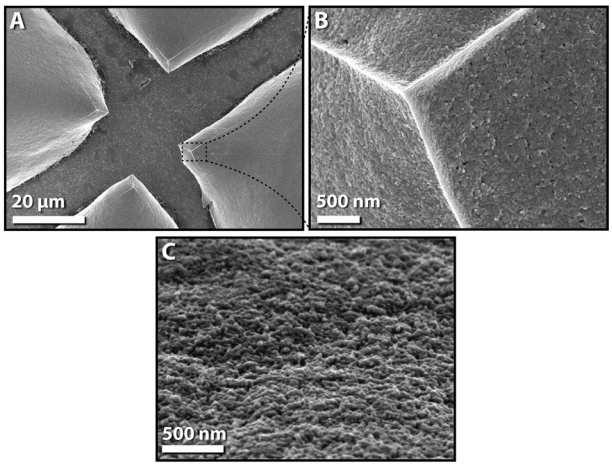

Figure 2. SEM images of supported MoP. A, B) MoP forms a dense thin film on the Ti foil. C) The surface of MoP displays a grainy nanostructured surface.

Scanning electron microscopy (SEM) shows that the as-synthesized MoP catalyst forms a dense thin film on the Ti foil with some cracking induced by the high-temperature reduction step during synthesis (Figure 2 A and B). A further magnification of the SEM image reveals a grainy nanostructured surface for MoP (Figure 2 C). No differences in sample morphology were observed after the sulfidation treatment for converting MoP into MoP | S (Figure S1), a point that will facilitate direct comparisons of their catalytic activities.

The chemical nature of as-prepared MoP and MoP | S was further investigated by X-ray photoelectron spectroscopy (XPS; Figure 3). Deconvolution of the Mo 3d region by peak fitting for both MoP and MoP | S revealed a predominant

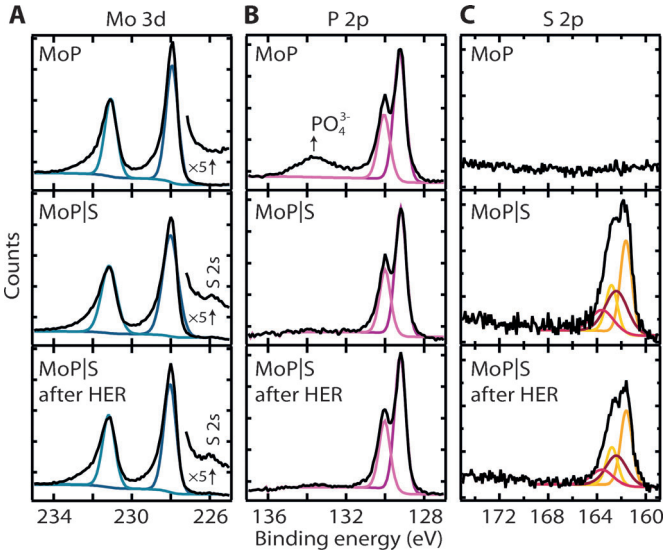

Figure 3. XPS spectra and fitted peaks of as-prepared MoP, MoP | S, and MoP | S after HER testing. A) Deconvolution of the Mo 3d region indicates that a molybdenum phosphide is present in all three materials. B) The predominant doublet found in the P 2p region can be assigned to P bonded to Mo (i.e., phosphide). C) The S 2p region for the two MoP | S samples can be fitted with two distinct doublets ($2p_{3/2}$, $2p_{1/2}$): one doublet (in yellow) that arises from sulfide species (S^{2-}) and one doublet (in red) from thiolate-type sulfur species.

Mo 3d doublet (228.2 eV, 231.3 eV) indicative of a $Mo^{\delta+}$ species ($0 < \delta \leq 4$) generally assigned to molybdenum in a molybdenum phosphide.[24,26,27]

The doublet in the P 2p region (129.4 eV, 130.2 eV) shows that the predominant P species in the surface of both MoP and MoP | S can be assigned to P bonded to Mo in the form of a phosphide.[24,26–27] In the case of MoP, an additional broad peak at 133.8 eV was observed, indicating a surface PO_4^{3-} species, likely produced upon exposure of the catalyst to air. Interestingly, in the case of MoP | S, this peak is not observable, an important point that we will return to shortly.

For the MoP | S sample, XPS further revealed the presence of sulfur at the surface by means of a small S 2s peak next to the Mo $3d_{5/2}$ peak and a stronger S 2p line, which can be deconvoluted into two distinct doublets ($2p_{3/2}$, $2p_{1/2}$): 1) one doublet (161.8 eV, 163.0 eV) that arises from a sulfide species (S^{2-}), and 2) one doublet (162.6 eV, 163.7 eV) indicative of sulfur in a thiolate-type environment. These sulfur species are similar to the ones observed for the phosphosulfides investigated for the HDS reaction.[24] It was determined by XPS that at the surface, sulfur accounts for 24 ± 3 % of the total amount of sulfur and phosphorus atoms. No oxygenated sulfur species such as sulfate were observed by XPS. We further performed a composition depth profile analysis using XPS by means of argon sputtering (see Figure S2), which revealed that sulfur is only present in approximately the topmost 10 nm of the film, confirming that the post-sulfidation treatment only creates a phosphosulfide at the surface, leaving the bulk of the catalyst intact as MoP.

The catalytic activities of MoP and MoP | S were evaluated for the HER using a three-electrode electrochemical

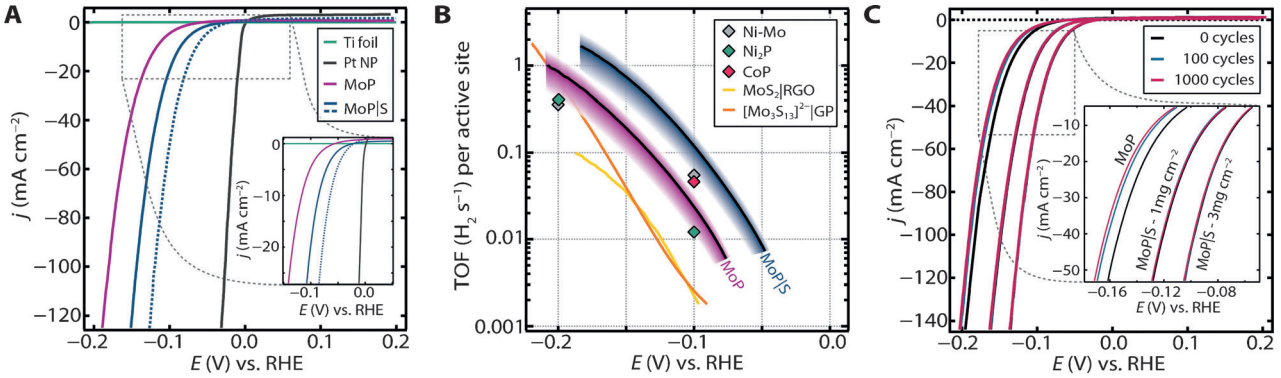

Figure 4. HER activity of MoP | S. A) Linear sweep voltammograms of MoP and MoP | S. The solid and dotted lines represent samples with loading of approximately 1 and 3 mg cm^{-2}, respectively. The HER activity of Pt nanoparticles (NP) is displayed for comparison. B) TOF values of MoP and MoP | S together with TOFs for Ni-Mo,[6] Ni_2P,[7] CoP,[8] MoS_2,[10] and $[Mo_3S_{13}]^{2-}$ [11] catalysts. For MoP and MoP | S, the black line represent a TOF value calculated using 40 μF cm^{-2} as the specific capacitance standard, and the borders of the colored gradients represent using 20 and 60 μF cm^{-2} for a lower and upper limit. MoP | S exhibits one of the highest TOF values of any non-precious-metal HER catalyst synthesized by a scalable route. C) Accelerated stability test. Initial and post-potential-cycling linear sweep voltammograms of MoP with an approximate loading of 1 mg cm^{-2} and of MoP | S with approximate loadings of 1 and 3 mg cm^{-2}. Whereas MoP experiences a slight decrease in current density upon increased potential cycling, MoP | S remains perfectly stable.

cell (conditions for all electrochemical experiments: H_2-purged H_2SO_4 (aq, 0.5 M), 23 °C, sweep rate: 5 mV s^{-1}, reference electrode: Hg | Hg_2SO_4 (sat. K_2SO_4), and counter electrode: graphite rod). Anodic-going iR-corrected linear sweep voltammograms for a bare Ti foil and for the supported MoP and MoP | S catalysts, which were normalized to the projected geometric area of the electrode, are shown in Figure 4 A (for Tafel plots and exchange current densities, j_0, see Figure S5). For reference, the cathodic-going sweeps are presented in Figure S3. Measurements of the Faradaic efficiency showed that essentially all of the current is used for H_2 evolution (Figure S4). The bare Ti foil shows no measurable HER activity within the investigated potential window. MoP with a loading of approximately 1 mg cm^{-2}, however, shows excellent catalytic activity for the HER, as indicated by the sharp increase in the magnitude of the cathodic current density with increasing overpotential, reaching 10 mA cm^{-2} and 100 mA cm^{-2} at overpotentials of 117 mV and 180 mV, respectively. We note that this activity for MoP is substantially higher than that of previously reported crystalline MoP catalysts, which produced a current density of 10 mA cm^{-2} at an overpotential of 125–150 mV at similar mass loadings.[19,20]

MoP is clearly a highly active HER catalyst, in particular for non-precious metals. Creating a surface phosphosulfide, however, substantially improves the activity over that of pure MoP, reducing the overpotential required to reach 10 mA cm^{-2} to only 86 mV for samples of similar loadings (Figure 4 A). Interestingly, amorphous MoP nanoparticles (1 mg cm^{-2}) tested immediately after annealing in H_2 (5 %)/Ar (95 %) show comparable activity to MoP | S with an overpotential of 90 mV for 10 mA cm^{-2}.[21] The overall activity of MoP | S can be further improved with higher loadings; with a loading of approximately 3 mg cm^{-2} of MoP | S, an overpotential of only 64 mV is required to reach 10 mA cm^{-2}, 78 mV to reach 20 mA cm^{-2}, and only 120 mV to reach 100 mA cm^{-2}. These values represent extraordinary electrode activities for the HER, particularly for non-precious-metal materials in acid. For comparison, the best performing molybdenum sulfide based electrodes require overpotentials greater than 100 mV to reach 10 mA cm^{-2}.[10,11,28–31] For a direct comparison to precious metals, the activity of Pt nanoparticles (ca. 3 nm diameter, supported on carbon with a Pt loading of 25 μg cm^{-2}) is also shown in Figure 4 A.

Stability is also a key concern for all catalysts. To assess the HER stability of MoP and MoP | S, we measured 1000 continuous cyclic voltammograms between −0.3 and 0.2 V versus the reversible hydrogen electrode (RHE; not iR-corrected) at 100 mV s^{-1}. This type of accelerated durability test is designed to represent the cycling expected for water (photo)electrolysis powered by intermittent renewable resources. Figure 4 C shows the iR-corrected anodic-going sweeps (10 mV s^{-1}) for three particular voltammograms: the initial cycle (0) and the 100th and 1000th stability cycles. For MoP, we observed a slight decrease in activity with increased potential cycling; after 1000 cycles, an additional overpotential of approximately 10 mV is needed to reach current densities of 10 and 100 mA cm^{-2}. Considering the corrosive nature of the strongly acidic environment, this is considered a fairly stable performance among non-precious-metal catalysts.[6,7] MoP | S, however, exhibited superb stability throughout this durability test, with overpotentials increasing by no more than 1 mV even at the highest current densities examined, >100 mA cm^{-2}. Galvanostatic stability measurements further demonstrated the outstanding stability of MoP | S (see Figure S6). Overall, these results show that introducing a surface phosphosulfide enhances both the catalytic activity and stability in a significant manner.

At this stage, reasons for the high activity and stability of the MoP | S catalyst are not entirely clear, and future work will aim to elucidate their origins. Mixed-metal alloy catalysts are well-known, but MoP | S represents a much less common mixed-anion catalyst. Our observations suggest that S and P

tune each other's electronic properties substantially to produce an active catalyst phase. Evidence of such a synergistic effect is found in the electrochemical and spectroscopic data. For instance, in the cyclic voltammogram of MoP shown in Figure S3, we observed hysteresis in the HER measurements for the cathodic-going and anodic-going sweeps, along with a broad redox feature between −0.05 and 0.15 V versus RHE, which is similar to a redox feature that was observed for Ni_2P.[7] This is indicative of a surface redox process involving MoP itself, potentially involving the surface PO_4^{3-}, which we observed with XPS. If such a species was reduced during the cathodic-going sweep, it could produce a more active state of the catalyst for the anodic-going sweep, explaining hysteresis in the HER data. A low degree of surface oxidation is also likely to be the origin of the very high activity of the amorphous MoP nanoparticles, as exposing these samples to ambient conditions reduced the activity significantly.[21] Interestingly, for MoP | S, there is minimal hysteresis and no evidence of any redox features (see Figure S3). The incorporation of sulfur into the surface apparently mitigates surface oxidation of the phosphide, consistent with our XPS measurements, which showed no PO_4^{3-} or SO_4^{2-} in the case of MoP | S after exposure to air or after HER catalysis; the two spectra are identical (Figure 3). Both spectroscopically and electrochemically, MoP | S appears to be a very stable HER catalyst in acid.

In catalysis, the best figure of merit to compare the intrinsic activities of different catalyst materials is by means of their turnover frequency (TOF), that is, the number of H_2 molecules evolved per second per active site.[32] The number of active sites was inferred from the electrochemically active surface area (ECSA), and as the exact number and nature of hydrogen binding sites is not known, we estimated the number of active sites as the number of surface sites including both Mo and P atoms as possible active sites (see the Supporting Information for details on the calculation of the TOF values). Figure 4C shows the TOF values of both MoP and MoP | S plotted against the applied potential together with the values for five state-of-the-art non-precious-metal HER catalysts, which were synthesized by a scalable route that was recently published: Ni-Mo nanopowder,[6] Ni_2P[7] and CoP[8] nanoparticles, MoS_2 nanoparticles supported on reduced graphene oxide (RGO),[10] and $[Mo_3S_{13}]^{2-}$ nanoclusters supported on high-surface-area graphite paper (GP).[11] The TOF values of Ni-Mo, CoP, and Ni_2P were estimated from the surface areas and crystal structures, similar to the present work, and the TOF values for RGO-supported MoS_2 and the $[Mo_3S_{13}]^{2-}$ nanoclusters were estimated per Mo atom based on the mass loadings.[11]

Both MoP and MoP | S exhibit very high catalytic activities for the HER. At overpotentials of 100 mV and 150 mV, the TOF values of MoP are 0.024 $H_2 s^{-1}$ and 0.19 $H_2 s^{-1}$, respectively. MoP | S displays even higher TOFs of 0.12 $H_2 s^{-1}$ and 0.75 $H_2 s^{-1}$, respectively. It is noteworthy that the measured roughness factors of approximately 300–400 seem extremely high considering the dense thin-film morphology of MoP and MoP | S as observed by SEM; this roughness factor is equivalent to that calculated for 20 nm Ni_2P particles.[7] Taking this into account and recalling that the depth profile revealed that most of the phosphosulfide resides within only approximately 10 nm of the surface, we suggest that the roughness factors used to calculate the TOFs reported here yield a conservative estimate; the true TOF could potentially be even higher. These values are among the highest reported TOFs of any scalable high-surface-area non-precious-metal HER catalyst, investigated either in acid or in base. For comparison, the Pt nanoparticles shown in Figure 4A display TOFs of 10 $H_2 s^{-1}$ and 100 $H_2 s^{-1}$ at overpotentials of only 7 mV and 36 mV, respectively.

We note that there is room for improvement in terms of the geometric-area activity. Both the MoP and MoP | S samples synthesized herein have not been deliberately modified for high surface areas, for example, by nanostructuring or by using high-surface-area supports; therefore, there is potential to improve performance even further on a geometric-area basis. Further studies are in progress to explore the nature of the high catalyst activities of MoP and MoP | S. The commonalities between HDS and HER also suggest that introducing a surface phosphosulfide onto other metals or metal alloy combinations could have a profound effect in increasing activity and/or stability even further. The results presented herein are important advances towards the development of an earth-abundant analogue to platinum for catalyzing the hydrogen evolution reaction in acid.

Received: August 17, 2014
Revised: September 25, 2014
Published online: October 30, 2014

Keywords: electrocatalysis · electrochemistry · hydrogen evolution reaction · molybdenum phosphide · phosphosulfide

[1] U.S. Energy Information Administration, The Impact of Increased Use of Hydrogen on Petroleum Consumption and Carbon Dioxide Emissions, **2008**.
[2] Z. Chen, T. F. Jaramillo, T. G. Deutsch, A. Kleiman-Shwarsctein, A. J. Forman, N. Gaillard, R. Garland, K. Takanabe, C. Heske, M. Sunkara, E. W. McFarland, K. Domen, E. L. Miller, J. A. Turner, H. N. Dinh, *J. Mater. Res.* **2010**, *25*, 3–16.
[3] M. G. Walter, E. L. Warren, J. R. McKone, S. W. Boettcher, Q. Mi, E. A. Santori, N. S. Lewis, *Chem. Rev.* **2010**, *110*, 6446–6473.
[4] T. R. Cook, D. K. Dogutan, S. Y. Reece, Y. Surendranath, T. S. Teets, D. G. Nocera, *Chem. Rev.* **2010**, *110*, 6474–6502.
[5] Y. Choquette, L. Brossard, A. Lasia, H. Ménard, *Electrochim. Acta* **1990**, *35*, 1251–1256.
[6] J. R. McKone, B. F. Sadtler, C. A. Werlang, N. S. Lewis, H. B. Gray, *ACS Catal.* **2013**, *3*, 166–169.
[7] E. J. Popczun, J. R. McKone, C. G. Read, A. J. Biacchi, A. M. Wiltrout, N. S. Lewis, R. E. Schaak, *J. Am. Chem. Soc.* **2013**, *135*, 9267–9270.
[8] E. J. Popczun, C. G. Read, C. W. Roske, N. S. Lewis, R. E. Schaak, *Angew. Chem. Int. Ed.* **2014**, *53*, 5427–5430; *Angew. Chem.* **2014**, *126*, 5531–5534.
[9] T. F. Jaramillo, K. P. Jørgensen, J. Bonde, J. H. Nielsen, S. Horch, I. Chorkendorff, *Science* **2007**, *317*, 100–102.
[10] Y. Li, H. Wang, L. Xie, Y. Liang, G. Hong, H. Dai, *J. Am. Chem. Soc.* **2011**, *133*, 7296–7299.
[11] J. Kibsgaard, T. F. Jaramillo, F. Besenbacher, *Nat. Chem.* **2014**, *6*, 248–253.

[12] J. Kibsgaard, Z. Chen, B. N. Reinecke, T. F. Jaramillo, *Nat. Mater.* **2012**, *11*, 963 – 969.
[13] H. Vrubel, D. Merki, X. Hu, *Energy Environ. Sci.* **2012**, *5*, 6136 – 6144.
[14] H. T. Wang, Z. Y. Lu, S. C. Xu, D. S. Kong, J. J. Cha, G. Y. Zheng, P. C. Hsu, K. Yan, D. Bradshaw, F. B. Prinz, Y. Cui, *Proc. Natl. Acad. Sci. USA* **2013**, *110*, 19701 – 19706.
[15] P. Liu, J. A. Rodriguez, *J. Am. Chem. Soc.* **2005**, *127*, 14871 – 14878.
[16] B. Hinnemann, P. G. Moses, J. Bonde, K. P. Jørgensen, J. H. Nielsen, S. Horch, I. Chorkendorff, J. K. Nørskov, *J. Am. Chem. Soc.* **2005**, *127*, 5308 – 5309.
[17] P. G. Moses, B. Hinnemann, H. Topsøe, J. K. Nørskov, *J. Catal.* **2007**, *248*, 188 – 203.
[18] C. G. Morales-Guio, L.-A. Stern, X. Hu, *Chem. Soc. Rev.* **2014**, *43*, 6555 – 6569.
[19] X. Wang, P. Xiao, L. Thia, M. Alam Sk, R. J. Lim, X. Ge, J.-Y. Wang, K. H. Lim, *Energy Environ. Sci.* **2014**, *7*, 2624 – 2629.
[20] Z. Xing, Q. Liu, A. M. Asiri, X. Sun, *Adv. Mater.* **2014**, *26*, 5702 – 5707.
[21] J. M. McEnaney, J. C. Crompton, J. F. Callejas, E. J. Popczun, A. J. Biacchi, N. S. Lewis, R. E. Schaak, *Chem. Mater.* **2014**, *26*, 4826 – 4831.
[22] Y. Shu, S. T. Oyama, *Carbon* **2005**, *43*, 1517 – 1532.
[23] R. Prins, M. E. Bussell, *Catal. Lett.* **2012**, *142*, 1413 – 1436.
[24] J. Bai, X. Li, A. Wang, R. Prins, Y. Wang, *J. Catal.* **2013**, *300*, 197 – 200.
[25] S. Rundqvist, T. Lundstrom, *Acta Chem. Scand.* **1963**, *17*, 37 – 46.
[26] D. C. Phillips, S. J. Sawhill, R. Self, M. E. Bussell, *J. Catal.* **2002**, *207*, 266 – 273.
[27] I. I. Abu, K. J. Smith, *J. Catal.* **2006**, *241*, 356 – 366.
[28] A. B. Laursen, P. C. K. Vesborg, I. Chorkendorff, *Chem. Commun.* **2013**, *49*, 4965 – 4967.
[29] H. Wang, Z. Lu, D. Kong, J. Sun, T. M. Hymel, Y. Cui, *ACS Nano* **2014**, *8*, 4940 – 4947.
[30] D. J. Li, U. N. Maiti, J. Lim, D. S. Choi, W. J. Lee, Y. Oh, G. Y. Lee, S. O. Kim, *Nano Lett.* **2014**, *14*, 1228 – 1233.
[31] J. D. Benck, T. R. Hellstern, J. Kibsgaard, P. Chakthranont, T. F. Jaramillo, *ACS Catal.* **2014**, *4*, 3957 – 3971.
[32] M. Boudart, *Chem. Rev.* **1995**, *95*, 661 – 666.

